Available online at www.sciencedirect.com
SCIENCE DIRECT®
Journal of Magnetic Resonance 179 (2006) 199–205
JMR Journal of Magnetic Resonance
www.elsevier.com/locate/jmr

Spin relaxation measurements of electrostatic bias in intermolecular exploration

Ching-Ling Teng, Robert G. Bryant *

Chemistry Department, Biophysics Program, University of Virginia, Charlottesville, VA 22904-4319, USA

Received 10 August 2005; revised 9 December 2005
Available online 28 December 2005

Abstract

We utilize the paramagnetic contribution to proton spin–lattice relaxation rate constants induced by freely diffusing charged paramagnetic centers to investigate the effect of charge on the intermolecular exploration of a protein by the small molecule. The proton NMR spectrum provided 255 resolved resonances that report how the explorer molecule local concentration varies with position on the surface. The measurements integrate over local dielectric constant variations, and, in principle, provide an experimental characterization of the surface free energy sampling biases introduced by the charge distribution on the protein. The experimental results for ribonuclease A obtained using positive, neutral, and negatively charged small nitroxide radicals are qualitatively similar to those expected from electrostatic calculations. However, while systematic electrostatic trends are apparent, the three different combinations of the data sets do not yield internally consistent values for the electrostatic contribution to the intermolecular free energy. We attribute this failure to the weakness of the electrostatic sampling bias for charged nitroxides in water and local variations in effective translational diffusion constant at the water–protein interface, which enters the nuclear spin relaxation equations for the nitroxide–proton dipolar coupling.

Keywords: Electrostatic; Potential; Diffusion; Charge distribution; Magnetic relaxation

The electron–nuclear dipole–dipole coupling between a paramagnetic center and the protons of a cosolute molecule is strongly dependent on the intermoment distance, which provides an experimental basis for characterizing proximity of one molecule to another. Several laboratories have applied this approach to characterization of intermolecular exploration in aqueous solutions [1–18]. When the diffusing paramagnet is charged, the interactions with the macromolecular surface are biased by the electrostatic fields created by the spatially dependent electrostatic potential of the macromolecule. Electrostatic contributions to intermolecular free energies may be significant determinants of molecular recognition and protein function [19–25].

The charge distributions in proteins have been the subject of considerable study, and there are several approaches available for computing them [26–29]. The effects of electrostatic interactions on the nuclear magnetic relaxation are indistinguishable from a steady state concentration gradient from a point on the solute molecule [30–34]:

$$[\mathrm{S}](r) = [\mathrm{S}]_o \mathrm{e}^{-\Phi(r)/k_\mathrm{B}T}, \tag{1}$$

where $\Phi(r)$ is the potential of mean force between the protein charge and the charged paramagnetic cosolute. The electrostatic interactions between the protein and the diffusing charged paramagnet molecules cause a nonuniform spatial distribution of the charged paramagnetic molecules. As discussed in detail for neutral diffusing paramagnetic centers, the nuclear spin–lattice relaxation rate is proportional to the effective local concentration of the paramagnet [17,18,35]. Thus, a comparison of the paramagnetic effects of positive, negative, and neutral paramagnetic centers on the protein proton relaxation rate constants may provide an experimental measure of the electrostatic potential sensed by the charged species at the protein–water

* Corresponding author. Fax: +1 804 924 3567.
E-mail address: rgb4g@virginia.edu (R.G. Bryant).

1090-7807/$ - see front matter © 2005 Elsevier Inc. All rights reserved.
doi:10.1016/j.jmr.2005.12.001

interface. In the absence of binding interactions, the motion of the paramagnetic centers is purely diffusive and the paramagnetic contribution to nuclear spin–lattice relaxation constant may be written [33,36],

$$\frac{1}{T_{1P}} = \frac{32\pi}{405}\gamma_I^2\gamma_S^2\hbar^2 S(S+1)\frac{N_A f}{1000} \times \frac{[S]}{bD}\{j_2(\omega_S-\omega_I)+3j_1(\omega_I)+6j_2(\omega_I+\omega_S)\}, \quad (2)$$

where $j(\omega) = \dfrac{1+\frac{5z}{8}+\frac{z^2}{8}}{1+z+\frac{z^2}{2}+\frac{z^3}{6}+\frac{4z^4}{81}+\frac{z^5}{81}+\frac{z^6}{648}}$; and $z = \left\{\frac{2\omega b^2}{D}\right\}^{1/2}$.

N_A is the Avogadro's constant, f is a steric factor, [S] is the molar concentration of electron spins, b is the the distance of closest approach between the electron and nuclear spin, D the relative translational diffusion constant, and ω is the Larmor frequency of the electron (S) or the nuclear spin (I). The paramagnetic contribution to the proton relaxation rate constant is thus proportional to the electron spin concentration [S], the translational correlation time, which is proportional to $1/D$, and the reciprocal of the distance of closest approach, b. If the translational correlation times for the electron–nuclear couplings are the same and dominated by the rapid motion of the radical, the paramagnetic contributions to the proton spin–lattice relaxation rate constants are proportional to local concentrations or concentration differences that are in turn caused by the electrostatic potential differences. Thus

$$\Delta G_j^{AB} = -RT\ln\frac{\left(\frac{1}{T1j}\right)_{\text{para}}^{\text{charge } A}}{\left(\frac{1}{T1j}\right)_{\text{para}}^{\text{charge } B}} = -zF\Phi_j, \quad (3)$$

where ΔG^{AB} is the Gibbs free energy difference associated with the difference in charge A and B, F is the faraday constant, z is the charge difference on the diffusing paramagnets, Φ the electrostatic potential difference, j identifies the observed proton site of the measurement, and the paramagnetic contribution to the relaxation rate constant is obtained from the differences between paramagnetic and diamagnetic solutions at the same concentrations

$$\left(\frac{1}{T_{1j}}\right)_{\text{para}} = \frac{1}{T_{1,j,\text{paramagnetic}}} - \frac{1}{T_{1,j,\text{diamagnetic}}}. \quad (4)$$

Although the dipole–dipole coupling falls rapidly with distance, for intermolecular relaxation modulated by diffusive motions, the distance dependence is much weaker than for intramolecular relaxation modulated by rotational diffusion at constant distance. Fig. 1 shows the fraction of the total paramagnetic relaxation contribution as a function of the distance of closest approach to the detected proton. More than 90% of the relaxation is induced within the first 10 Å of van der Waals contact for the nitroxide oxygen. However, in the present context, the electrostatic bias introduced by the diffusing paramagnet is carried by the charged group, which is at the opposite end of the nitroxide molecule from the paramagnetic center. This is nearly 10 Å away, and if the molecule approaches the protein with the charged end in contact, the relaxation contribution from this orientation is small, of order 5–10% of that for nitroxide end contact. Therefore, the electrostatic bias sensed by the paramagnetic relaxation contribution to the protons modulated by relative diffusive motion of these nitroxide explorer molecules, is dominated by the nitroxide contact orientation, which places the charged group well into the high dielectric aqueous environment. While the electrostatic bias is not eliminated as a consequence, it is significantly attenuated compared with the case where the center of charge and the paramagnetic center coincide.

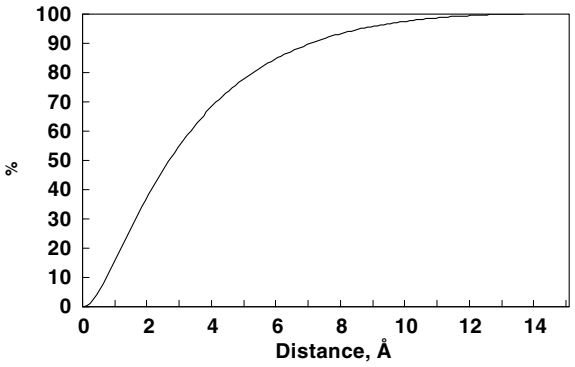

Fig. 1. The fraction of the total paramagnetic relaxation rate induced at a detected proton spin as a function of the distance from the nitroxide starting at the closest approach or van der Waals contact. The calculation assumes that the electron spin–lattice relaxation time is infinite and that closest approach corresponds to an intermoment distance of 3.5 Å. The relative translational diffusion constant was assumed to be 4×10^{-6} cm^2 s^{-1} [38].

1. Experimental

The nitroxides, 4-carboxy-TEMPO, 4-amino-TEMPO, and 4-hydroxy-TEMPO were obtained from Aldrich Chemical, St. Louis, MO. Thin layer chromatography using silica gel and methanol–chloroform mixtures showed that generally these compounds had several components as supplied. Recrystallization improved purity; however, the nitroxide solutions may differ slightly in radical concentration. To minimize the effects of such small concentration differences, the paramagnetic contribution to the water proton relaxation rate was measured in each solution. The water proton relaxation rate constant is determined by the relative diffusive motion of the nitroxide and the water molecules, and is linear in the nitroxide spin concentration. The relaxation data for the protein protons were normalized to the nitroxide induced water proton relaxation rate to minimize any variations from small differences in radical concentration.

All NMR data were acquired using a 500 MHz Varian Unity Plus spectrometer as previously described. The ribonuclease A concentration was 4.0 mM and measurements were made at 35 °C and pH 7.5 and a nitroxide concentration of 5.0 mM. Both the protein and nitroxide concentrations were calibrated by UV–Vis absorption. Measurement

errors in spin–lattice relaxation rates are a function of the width of the cross-peak utilized as well as the spin–lattice relaxation rate constant measured. The errors propagate in these measurements because the free energy difference is deduced from the logarithm of the ratio of differences in relaxation rate constants; i.e., three measurements are involved. If variations in translational diffusion were unimportant, we estimate that the mean errors in the free energies deduced are approximately 10%.

2. Results and discussion

The distribution of paramagnetic contributions to the protein proton spin–lattice relaxation rate constants for all 255 spectrally resolved protein resonances is shown in Fig. 2 for 4-carboxy-TEMPO, 4-amino-TEMPO, and 4-hydroxy-TEMPO. The magnitudes of the paramagnetic relaxation rate contributions are in the range expected for electron–nuclear relaxation correlated by relative translational diffusion. The distribution of the relaxation rate changes caused by uncharged 4-hydroxy-TEMPO is narrower and has no rate changes greater than 3.3 s^{-1}, while the charged nitroxide data show several protons with relaxation rate constants larger than 3.3 s^{-1}. This difference suggests that there are stronger interactions for some protons with the charged nitroxides.

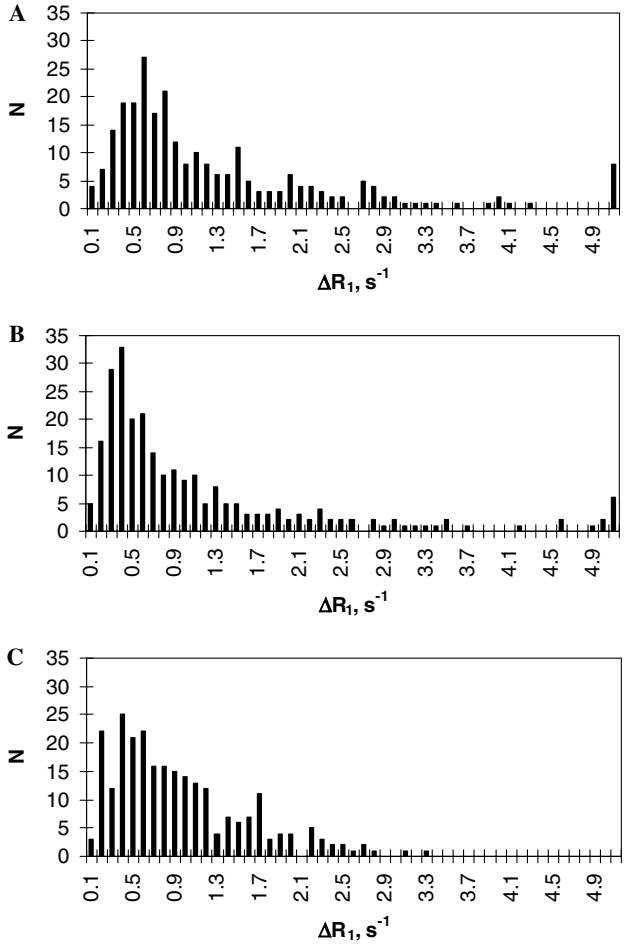

Fig. 2. The paramagnetic contribution to the proton relaxation rate constants for 255 spectrally resolved ribonuclease A at 4.0 mM in 5.0 mM solutions of (A) 4-amino-TEMPO, (B) 4-carboxy-TEMPO, and (C) 4-hydroxy-TEMPO at 25 °C and pH 7.5.

One might argue the paramagnetic rate enhancement is not caused by variations in local concentration, but rather, by weak binding interactions. However, we point out that were a nitroxide bound to the protein site for a time longer than the rotational correlation time of the protein or approximately 10 ns, the spin–lattice relaxation rate constant would be dominated by a rotationally correlated electron–nuclear coupling. For ribonuclease A, the classic Solomon, Bloembergen, and Morgan equations yield a spin–lattice relaxation rate constant of 2000 s^{-1} assuming the rotational correlation time of 5 ns and an intermoment distance of 3.0 Å. For the same parameters, the transverse relaxation rate constant is 3.3×10^5 s^{-1}, which corresponds to a proton linewidth of approximately 10,000 Hz. These calculations for a rotationally correlated electron–nuclear coupling associated with a bound nitroxide indicate that the few protons that have somewhat larger rates for the charged nitroxides do not suffer significant binding interactions because very large linewidths would make these protons unobservable. If a nitroxide bound to a particular site for a time long compared with the rotational correlation time of the protein and exchanged among protein molecules in a time short compared with the proton T_1 (of order 0.5 s), the weak binding would broaden the resonances in the binding region. If the binding probability is only 1%, then the linewidths would be of order of 100 Hz. Because the linewidth changes are substantially smaller, any binding interactions are substantially weaker than this, a conclusion supported by the absence of changes in the ESR spectrum (data not shown) [37]. Other aspects of the data support the contention that the electron–nuclear coupling is not rotationally correlated as discussed below.

The protein protons in the interior of the protein may be relaxed by the diffusing radicals directly, or by a pathway that involves spin-diffusion processes that may couple rapidly relaxed surface protons and interior protons. However, the proton–proton connectivity remains the same in the absence of conformational changes induced by the different radicals. The NMR spectrum implies that there are no conformational changes at the concentrations used; therefore, the effects of spin diffusion should be similar for the interior protons regardless of the charge on the paramagnet. The effect of spin diffusion may be assessed by comparing the paramagnetic contributions to the relaxation rate in geminal proton pairs. There are 39 geminal pairs in our data set. The distribution of the differences in paramagnetic rate enhancement in geminal proton pairs is shown in Fig. 3. The average difference in the paramagnetic contribution to the relaxation rate is ~50%, with some very large differences observed. The magnitude of the relaxation rate enhancement differences in geminal pairs suggests that spin

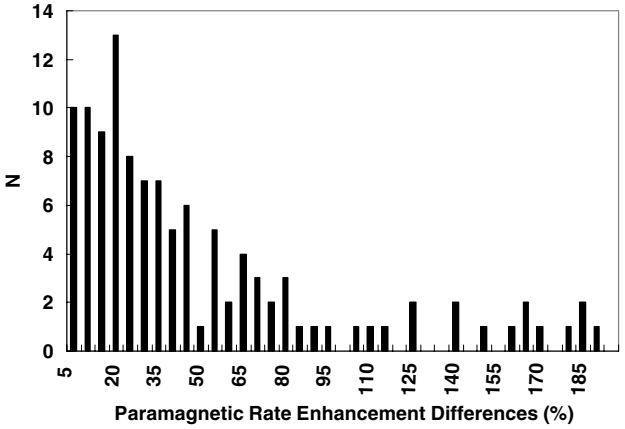

Fig. 3. The distribution for paramagnetic relaxation rate enhancements for the geminal proton pairs defined as the difference in the relaxation rate constants for the geminal protons divided by the mean of the two paramagnetic contributions.

diffusion is not the dominant factor influencing the relaxation rate measurements.

The effects of spin–spin communication are least for surface protons. The surface protons were operationally defined based on the crystal structure of the protein and the distance of closest approach, b, for the intermolecular electron–nuclear interaction of each protein proton. The protein surface was identified by computing the shortest distance between a proton and the calculated Connolly protein molecular surface defined by a surface probe of 1.4 Å radius (Molecular Simulations, San Diego, CA). A proton is counted as a surface proton if the distance of closest approach is 2.7 Å or shorter. This distance corresponds approximately to van der Waals contact between the oxygen of the nitroxides and a proton presuming that the electronic point magnetic dipole is midway between the oxygen and the nitrogen. There are 255 well resolved RNase A protons at pH 7.5 of which 136 are at the surface defined in this way.

The relaxation rate differences for surface protons between the paramagnetic samples and the diamagnetic samples are summarized for 4-amino-TEMPO, 4-carboxy-TEMPO, and 4-hydroxy-TEMPO in Fig. 4 for ribonuclease A at pH 7.5. The distributions are qualitatively similar. The paramagnetic contributions to the surface proton relaxation rate constants do not correlate with static accessible surface area (data not shown); the correlation coefficients, R^2, for 4-carboxy tempo and 4-amino-TEMPO are 0.03 and the slopes are 0.04 and 0.06, respectively. Therefore, factors other than random collisions with the surface protons contribute significantly to the observed relaxation induced by these paramagnetic compounds.

Fig. 5 shows the paramagnetic relaxation rate contribution from 4-hydroxy-TEMPO for interior protons in ribonuclease A defined as those protons with distances of closest approach greater than or equal to 2.8 Å. The two solid lines were computed based on the equation $1/T_{1\mathrm{para}} = \mathrm{Ar}^{-c}$. The flatter curve is a fit of the data with the value of

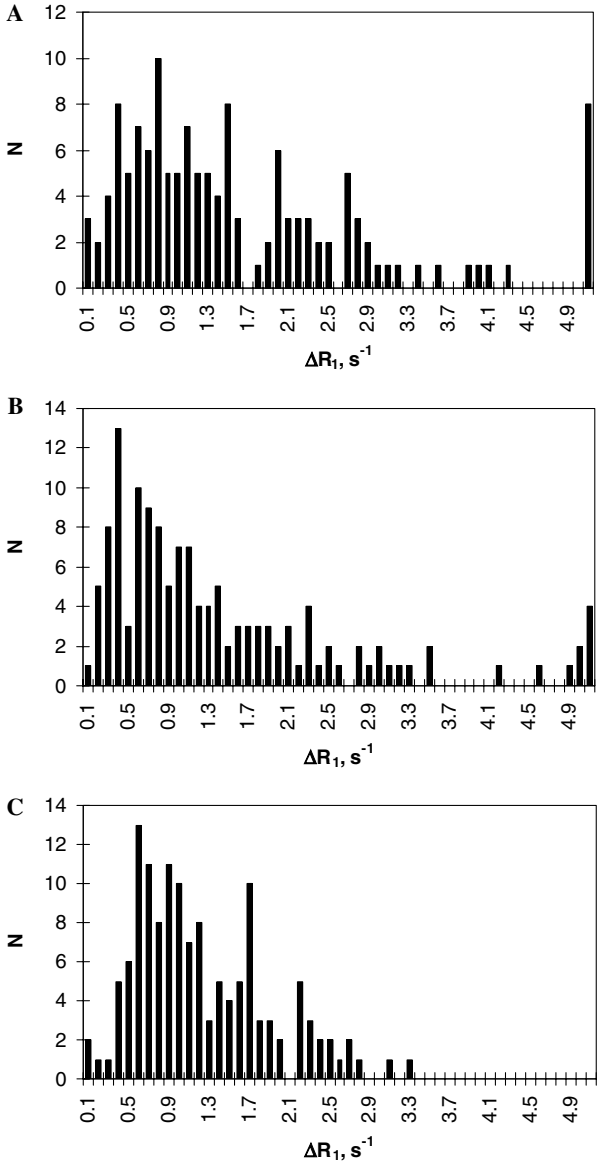

Fig. 4. The paramagnetic contribution to the proton relaxation rate constants for ribonuclease A surface protons defined by Eq. (4) in solutions of (A) 4-amino-TEMPO, (B) 4-carboxy-TEMPO, and (C) 4-hydroxy-TEMPO at 35 °C and pH 7.5

$c = 0.82$ and the value of R^2 only 0.09. The scatter in the data is large, but this slope is close to the value of -1 which is implied by Eq. (2). If the paramagnetic contributions had substantial rotational correlation associated with a dominant contribution from nitroxide binding, the value of c would be 6, which is shown as the steeper solid line in Fig. 5 and does not represent the data well. Thus, we conclude that rotational correlation is not a significant factor in the present data.

The scatter in Fig. 5 raises a serious concern about application of Eq. (3), which rests on the assumption that the translational correlation time for the diffusing nitroxides is uniform as sensed by all protons detected. Although the translational diffusion constant of the paramagnet enters the relaxation rate directly, the similar size of the

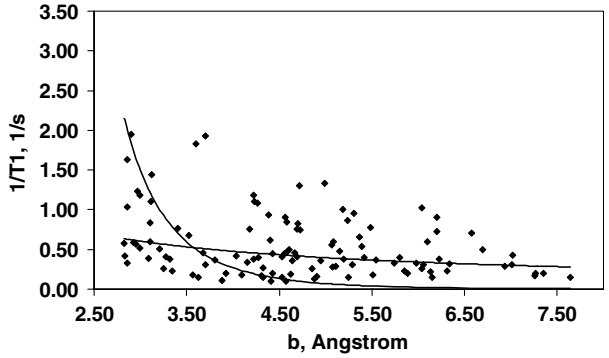

Fig. 5. The measured paramagnetic contribution to ribonuclease A protons which are 2.8 Å or farther away from the diffusing 4-hydroxy-TEMPO vs the distance of closest approach computed from the sum of van der Waals radii and the protein surface as defined in the text. The solid line with small slope is a fit to the equation $y = Ab^{-c}$ with $c = 0.83$ and $R^2 = 0.09$. The second solid line was computed with $c = 6$ for comparison.

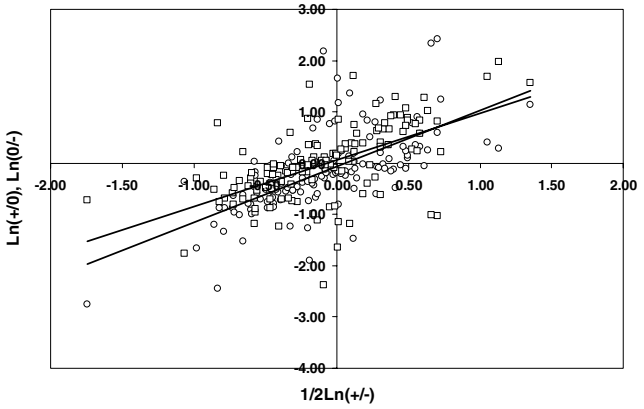

Fig. 6. Comparisons of the values of the free energy, in units of RT obtained from paramagnetic relaxation rate contributions according to Eq. (3). The cation/anion (+/−) comparison is taken as the reference and the cation to neutral (+/0) and the neutral to anion (0/−) values are then plotted against this reference. The solid lines are least squares fits to the anticipated linear correlation: the (+/0) slope is 0.91 with $R^2 = 0.35$; the (0/−) slope is 1.09 with $R^2 = 0.44$.

radicals used suggests that the differences in effective local diffusion constant would be small. This assumption is questionable. The significant deviations in relaxation rates shown in Fig. 5 imply that more than the intermoment distance affects the detected paramagnetic contribution to the relaxation rate constant. Local variations in effective translational diffusion constant of order a factor 3 are reasonable because of surface topography, counter ion effects, and heterogeneity in water–protein interactions. The data in Fig. 5 support the contention that this variation is significant. The surface protons show a much larger variation in relaxation rate.

The relaxation rates are proportional to the sum of intermolecular potentials that determine the effective local concentration and collision probabilities between the protons detected and the diffusing paramagnetic solutes. These factors may include particularly the effects of the electrostatic charge on the diffusing paramagnet. Because these radicals are closely related structurally, it is attractive to pursue the idea of taking the ratio of relaxation rate constant differences as indicated in Eq. (3) to provide the free energy difference associated with the charge differences rather than the other factors that affect proximity of to the detected protons. If the steric constraints associated with the accessibility to an individual proton are essentially the same for each radical comparison, the steric factors cancel. Although the several concerns expressed above cast doubt on the validity of any particular value for the free energy deduced on the basis of Eq. (3), it is instructive to examine its application.

Eq. (3) was applied to deduce free energy estimates from three combinations of data: (1) the comparison of the positive to the neutral radical, (2) the comparison of the neutral to the negatively charged radical, and (3) the comparison of the positive to the negatively charged radical. The three data sets are represented in Fig. 6 where the comparison of the positive to negative radical data sets are taken as the reference and the other two plotted against it. If the procedure produced a reliable measure of the electrostatic contribution to the free energy, the values would be the same regardless of which data comparison was used and the data would all fall on a straight line of slope 1. However, this is not the observation shown in Fig. 6. There are large deviations in the values computed using different data sets and there are cases where both oppositely charged nitroxides show stronger paramagnetic rate enhancement compared to that of a neutral nitroxide molecule. However, the linear regression lines for the two data sets have slopes near unity, which suggest that the electrostatic contribution is reflected in the aggregate of the measurements. It is in this spirit that we examine the distributions of free energies deduced in this way as shown in Fig. 7. The mean values of the free energy distributions are all nearly zero, consistent with a near cancellation of positive and negative regions of the protein at pH 7.5. However, the widths of the three distributions are different, with the (0/−) distribution 65% larger than the (+/−) distribution. The origin of this difference cannot be in the electrostatic contribution to the sampling bias of the explorer molecules because it should not matter which data set pair is used to make the comparison. Other factors, such as the changes in local translational diffusion constant caused by electrostatic interactions, must contribute.

To understand the origin of these poor correlations, it is useful to consider the size of the energetic contributions expected. If there is a unit charge on the explorer molecule 10 Å away from a point charge on the protein, then the electrostatic energy for the interacting charges is estimated to be of order 0.7 *RT* if the dielectric constant is 80. This value drops to 0.5 *RT* at 15 Å which is a relevant distance because the protons detected in these observations are not coincident with the charge. Thus, the electrostatic contributions to the free energy are small and on the order of other weak intermolecular contributions. This simple estimate

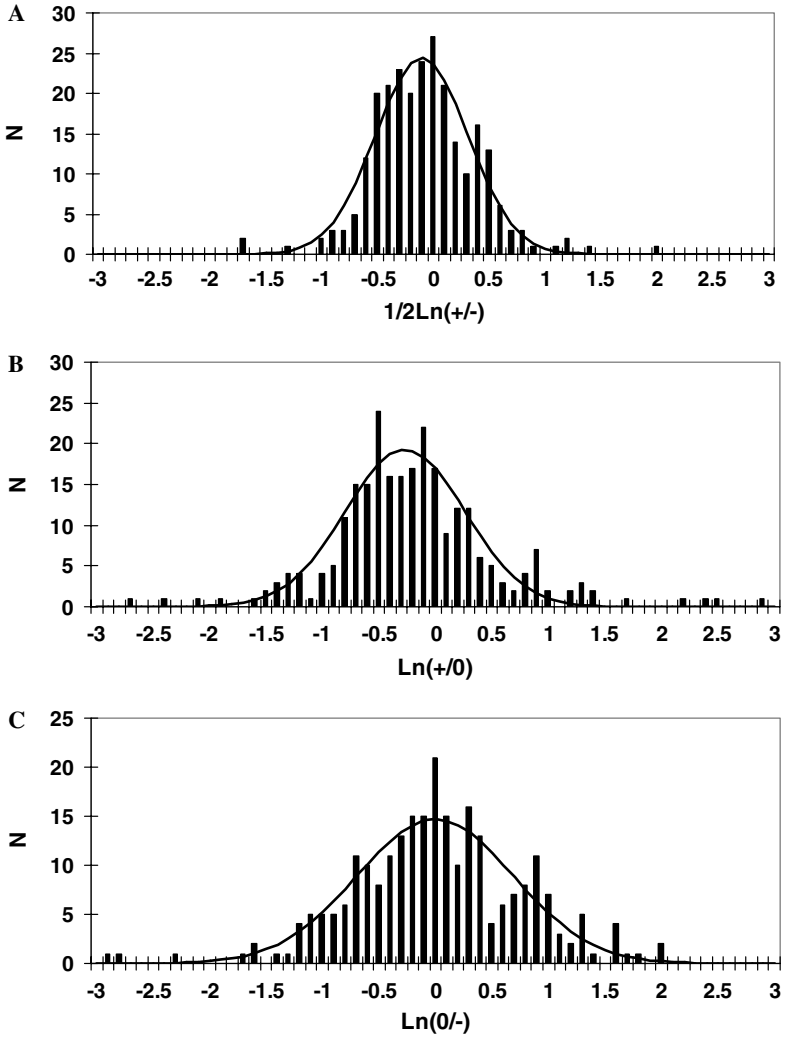

Fig. 7. Distributions of electrostatic free energy contributions deduced from nitroxide induced relaxation rate constants. The solid lines are best Gaussian fits: (A) 4-amino-TEMPO and 4-carboxy-TEMPO, the width is 0.42 and the mean −0.105; (B) 4 amino-TEMPO and 4-hydroxy-TEMPO, the width is 0.53 and the mean −0.270; (C) 4-hydroxy-TEMPO and 4-carboxy-TEMPO, the width is 0.693 and the mean −0.004.

shows that the values of the energy deduced by the spin-relaxation strategy are of reasonable magnitude. The small values show that the effective dielectric constant sensed by this set of charged explorer molecules is effectively that of water. Were the choice of a large dielectric constant inappropriate, the magnitude of the observed relaxation rate changes observed would be much larger.

3. Conclusion

The high resolution afforded by the NMR spectrum of a protein provides an experimental approach for detecting contributions to the intermolecular free energy differences between protein and a freely diffusing charged paramagnetic cosolute. The free energy values deduced from the experiments are small and in reasonable qualitative agreement with predictions of now standard computational approaches. While the magnitudes of the free energy values deduced using this measurement strategy are reasonable, the three different combinations of the data sets yield values that may differ substantially. We conclude that the confounding difficulties of a variable local translational diffusion constant provide errors that are too large to yield quantitatively reliable effective electrostatic potentials on proteins using relaxation probes like nitroxides with long electronic spin–lattice relaxation time constants and where the center of mass and charge do not coincide. The approach may be more successful using paramagnetic metal complexes with electron spin relaxation times in the several picosecond range which would effectively decouple the measurement of intermolecular proximity from the relative translational dynamics.

References

[1] G. Esposito, A.M. Lesk, H. Molinari, A. Motta, N. Niccolai, A. Pastore, Probing protein structure by solvent perturbation of nuclear magnetic resonance spectra. Nuclear magnetic resonance spectral editing and topological mapping in proteins by paramagnetic relaxation filtering, J. Mol. Biol. 224 (1992) 659–670.

[2] G. Esposito, A.M. Lesk, H. Molinari, A. Motta, N. Niccolai, A. Pastore, Probing protein structure by solvent perturbation of NMR spectra. II. Determination of surface and buried residues in homologous proteins, Biopolymers 33 (1993) 839–846.
[3] G. Hernandez, C.L. Teng, R.G. Bryant, D.M. LeMaster, O2 penetration and proton burial depth in proteins: applicability to fold family recognition, J. Am. Chem. Soc. 124 (2002) 4463–4472.
[4] P.A. Luchette, R.S. Prosser, C.R. Sanders, Oxygen as a paramagnetic probe of membrane protein structure by cysteine mutagenesis and (19)F NMR spectroscopy, J. Am. Chem. Soc. 124 (2002) 1778–1781.
[5] L. McNaughton, G. Hernandez, D.M. LeMaster, Equilibrium O_2 distribution in Zn^{2+}-protoporphyrin IX deoxymyoglobin mimic: application to oxygen migration pathway analysis, J. Am. Chem. Soc. 125 (2003) 3813–3820.
[6] H. Molinari, G. Esposito, L. Ragona, M. Pegna, N. Niccolai, R.M. Brunne, A.M. Lesk, L. Zetta, Probing protein structure by solvent perturbation of NMR spectra: the surface accessibility of bovine pancreatic trypsin inhibitor, Biophys. J. 73 (1997) 382–396.
[7] N. Niccolai, A. Ciutti, O. Spiga, M. Scarselli, A. Bernini, L. Bracci, D. Di Maro, C. Dalvit, H. Molinari, G. Esposito, P.A. Temussi, NMR studies of protein surface accessibility, J. Biol. Chem. 276 (2001) 42455–42461.
[8] N. Niccolai, V.G.C. Rossi, W. Gibbons, The stereochemistry and dynamics of natural products and biopolymers from proton relaxation spectroscopy: spin label delineation of inner and outer protons of Gramicidin S including hydrogen bonds, J. Am. Chem. Soc. 104 (1982) 1534–1537.
[9] N. Niccolai, R. Lampariello, L. Bovalini, M. Rustici, P. Mascagni, P. Martelli, Solvent spin-labelling for investigating the interaction of biological ligands with macromolecules. A ^1H paramagnetic relaxation study, Biophys. Chem. 38 (1990) 155–158.
[10] N. Niccolai, C. Rossi, G. Valensin, P. Mascagni, W.A. Gibbons, An investigation of the mechanisms of nitroxide-induced proton relaxation enhancements in biopolymers, J. Phys. Chem. 88 (1984) 5689–5692.
[11] N. Niccolai, R. Spadaccini, M. Scarselli, A. Bernini, O. Crescenzi, O. Spiga, A. Ciutti, D. Di Maro, L. Bracci, C. Dalvit, P.A. Temussi, Probing the surface of a sweet protein: NMR study of MNEI with a paramagnetic probe, Protein Sci. 10 (2001) 1498–1507.
[12] G. Otting, E. Liepinsh, B. Halle, U. Frey, NMR identification of hydrophobic cavities with low water occupancies in protein structures using small gas molecules, Nat. Struct. Biol. 4 (1997) 396–404.
[13] G. Pintacuda, G. Otting, Identification of protein surfaces by NMR measurements of a paramagnetic Gd(III) chelate, J. Am. Chem. Soc. 124 (2002) 372–373.
[14] R.S. Prosser, P.A. Luchette, P.W. Westerman, Using O_2 to probe membrane immersion depth by 19F NMR, Proc. Natl. Acad. Sci. USA 97 (2000) 9967–9971.
[15] R.S. Prosser, P.A. Luchette, P.W. Westerman, A. Rozek, R.E. Hancock, Determination of membrane immersion depth with O(2): a high-pressure (19)F NMR study, Biophys. J. 80 (2001) 1406–1416.
[16] C.L. Teng, R.G. Bryant, Experimental measurement of nonuniform dioxygen accessibility to ribonuclease a surface and interior, J. Am. Chem. Soc. 122 (2000) 2667–2668.
[17] C.L. Teng, R.G. Bryant, Mapping oxygen accessibility to ribonuclease a using high resolution NMR relaxation spectroscopy, Biophys. J. 86 (2004) 1713–1725.
[18] C.-L. Teng, S. Martini, R.G. Bryant, Local measures of intermolelcular free energies in aqueous solutions, J. Am. Chem. Soc. 126 (2004) 15253–15257.
[19] A. Warshel, S.T. Russell, Calculations of electrostatic interactions in biological systems and in solutions, Q. Rev. Biophys. 17 (1984) 283–422.
[20] J.B. Matthew, Electrostatic effects in proteins, Annu. Rev. Biophys. Biophys. Chem. 14 (1985) 387–417.
[21] J.A. McCammon, Theory of biomolecular recognition, Curr. Opin. Struct. Biol. 8 (1998) 245–249.
[22] K.A. Sharp, B. Honig, Electrostatic interactions in macromolecules: theory and applications, Annu. Rev. Biophys. Biophys. Chem. 19 (1990) 301–332.
[23] H. Nakamura, Roles of electrostatic interaction in proteins, Quarterly Reviews of Biophysics 29 (1996) 1–90.
[24] B.M. Fisher, L.W. Schultz, R.T. Raines, Coulombic effects of remote subsites on the active site of ribonuclease A, Biochemistry 37 (1998) 17386–17401.
[25] G.I. Likhtenshtein, I. Adin, A. Novoselsky, A. Shames, I. Vaisbuch, R. Glaser, NMR studies of electrostatic potential distribution around biologically important molecules, Biophysical Journal 77 (1999) 443–453.
[26] B. Honig, A. Nicholls, Classical electrostatics in biology and chemistry, Science 268 (1995) 1144–1149.
[27] B. Honig, K.A. Sharp, A.-S. Yang, Macroscopic models of aqueous solutions: biological and chemical applications, J. Phys. Chem. 97 (1993) 1101–1109.
[28] C.N. Schutz, A. Warshel, What are the dielectric constants of proteins and how to validate electrostatic models? Proteins 44 (2001) 400–417.
[29] N.A. Baker, J.A. McCammon, Electrostatic interactions, Methods Biochem. Anal. 44 (2003) 427–440.
[30] P.H. Fries, F.G. Jagannathan, F.G. Herring, G.H. Patey, The relative motion of ions in solution. II. An NMR relaxation study of attractive ions in water at low ionic strength, J. Chem. Phys. 80 (1984) 6267–6273.
[31] P.H. Fries, G.H. Patey, The relative motion of ions in solution. I. Microdynamical models and intermolecular dipolar spin relaxation, J. Chem. Phys. 80 (1984) 6253–6266.
[32] P.H. Fries, J. Rendell, E.E. Burnell, G.N. Patey, The relative motion of ions in solution. III. An NMR relaxation study of repulsive ions in water at low ionic strength, J. Chem. Phys. 83 (1985) 307–311.
[33] J.H. Freed, Dynamic effects of pair correlation functions on spin relaxation by translational diffusion in liquids. II. Finite jumps and independent T1 processes, J. Chem. Phys. 68 (1978) 4034–4037.
[34] T.R.J. Dinesen, J. Seymour, L. McGowan, S. Wagner, R.G. Bryant, F-19 and H-1 magnetic relaxation dispersion determination of the translational encounter between ionic salts and nitroxide free radicals in aqueous solution, J. Phys. Chem. A 103 (1999) 782–786.
[35] C.L. Teng, R.G. Bryant, Oxygen accessibility to ribonuclease A: quantitative interpretation of nuclear spin relaxation induced by a freely diffusing paramagnet. J. Phys. Chem. (in press) (2005).
[36] L. Hwang, J.H. Freed, Dynamic effects of pair correlation functions on spin relaxation by translational diffusion in liquids, J. Chem. Phys. 63 (1975) 4017–4025.
[37] C.L. Teng, Mapping molecular accessibility, in: Biophysics Program, University of Virginia, Charlottesville, VA, USA, 2002, p. 378.
[38] C.F. Polnaszek, R.G. Bryant, Nitroxide radical induced solvent proton relaxation: measurement of localized translational diffusion, J. Chem. Phys. 81 (1984) 4038–4045.